

## COMPARISON OF PEDOGENIC AND SEDIMENTARY GREIGITE BY X-RAY DIFFRACTION AND MÖSSBAUER SPECTROSCOPY

HELGE STANJEK AND ENVER MURAD\*

Lehrstuhl für Bodenkunde der Technischen Universität München  
D-85350 Freising-Weihenstephan, Germany

**Abstract**—Greigites from a gley and a Tertiary sediment were investigated by X-ray diffraction and Mössbauer spectroscopy. The cell-edge length  $a$  of  $9.8639 \text{ \AA} \pm 0.0003 \text{ \AA}$  for the soil greigite was significantly smaller than that of the sedimentary greigite ( $9.8737 \text{ \AA} \pm 0.0004 \text{ \AA}$ ), but both cell-edge lengths were smaller than the value given on JCPDS card #16-713 ( $9.876 \text{ \AA}$ ). Both greigites had 440 as strongest peak rather than 311 (as indicated on JCPDS card #16-713), but the other relative intensities did not deviate from the values given on this card within experimental error. Mean X-ray diffraction coherence lengths of  $23 \pm 2 \text{ nm}$  for the soil greigite and of  $60 \pm 5 \text{ nm}$  for the sedimentary greigite suggest superparamagnetic behavior. Mössbauer spectra nevertheless comprised two sextets with hyperfine fields of about 31.2 T (tetrahedral sites) and 30.7 T (octahedral sites), which resemble published values. It is postulated that aggregation may play an important role in determining the magnetic properties of the described samples.

**Key Words**—Greigite, Mössbauer, Sediment, Soil, XRD.

### INTRODUCTION

The ferrimagnetic mineral greigite ( $\text{Fe}^{2+}\text{Fe}_3^{2+}\text{S}_4$ ) has been described from marine, brackish and freshwater lacustrine sediments (Jedwab, 1967; Berner, 1969; Dell, 1972; Snowball, 1988; Mann *et al.*, 1990). In a recently described occurrence,  $\delta \text{S}^{34}$  isotope analyses and TEM observations indicated a greigite formed in a gley soil to be of biogenic origin (Stanjek *et al.*, 1994). Preliminary X-ray diffraction and TEM work indicate the mean particle size of this soil greigite to lie in the superparamagnetic region as defined by Ricci and Kirschvink (1992), but its macroscopic behavior corresponds to that of single-domain particles. In an attempt to elucidate this contradictory behavior, room-temperature Mössbauer spectra were taken of this soil greigite and of a sedimentary greigite from the Sokolov Basin in Western Bohemia (previously described by Hoffmann, 1992).

### MATERIALS AND METHODS

The soil greigite was formed in a gley developed from colluvial material eroded from the Hesselberg, Bavaria. The zone of greigite formation begins at a depth of about 70 cm ( $\text{Gr}_2$ ) and ends at about 100 cm in the  $\text{Gr}_3$  horizon. A detailed description of this occurrence has been given by Auerswald *et al.* (1992). The sedimentary greigite was extracted magnetically from Miocene claystones (for further details see Krs *et al.*, 1990).

X-ray diffraction analyses were carried out with a Huber Guinier diffractometer using  $\text{Co K}\alpha_1$  radiation.

Step scans were run from  $10^\circ$ – $100^\circ 2\theta$  with an increment of  $0.02^\circ$  and a counting time of 30 sec. Silicon powder with a particle size  $< 20 \mu\text{m}$  (Merck, #12497) with a unit-cell dimension  $a = 5.4307 \text{ \AA}$  (Klug and Alexander, 1974) served as an internal standard. The scans were fitted with a program based on the IR-spectra fitting program by Janik and Raupach (1977) and ported to C by Stanjek. In order to better approximate the peak shapes by the fitted Pseudo-Voigt functions, each greigite peak was fitted with three individual peaks. The program CDruk was used to sum up these single peaks to a combined peak from which the integral intensity and centroid were calculated. Peak intensities were corrected for the Lorentz- and polarization factor (De Wolf and Visser, 1988) but not for sample absorption. Instrumental broadening was determined using annealed  $\text{Fe}_2\text{O}_3$  and quartz. To calculate the effective particle size and strain, the measured integral widths were corrected for instrumental broadening by applying correction functions derived from folding procedures (Stanjek, 1991). Based on the postulation that particle-size broadening yields Lorentzian profiles and strain broadening Gaussian profiles, both effects can be separated by the formula given by Klug and Alexander (1974, p. 665):

$$\frac{(\delta 2\vartheta)^2}{\tan^2\vartheta_0} = \frac{K\lambda}{L} \left[ \frac{\delta 2\vartheta}{\tan\vartheta_0 \sin\vartheta_0} \right] + 16e^2 \quad (1)$$

where  $\delta 2\vartheta$  is the integral breadth corrected for instrumental broadening,  $\vartheta_0$  is the angle of reflection,  $K$  is the Scherrer constant,  $\lambda$  is the wavelength,  $L$  is the mean coherence length of the crystallites (MCL), and  $e$  is the strain.  $K$  was taken from Langford and Wilson (1978) assuming the crystallites to be octahedral in shape. A

\* Present address: Bayerisches Geologisches Landesamt, Concordiastrasse 28, D-96049 Bamberg, Germany.

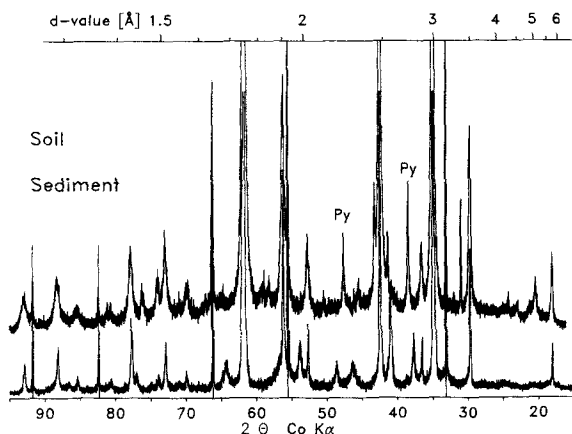


Figure 1. X-ray diffraction diagrams of soil (top) and sedimentary (bottom) greigites. Vertical lines indicate the internal standard Si. Py = Pyrite.

plot of the left side of the equation (Y in Figure 2) against the term in brackets on the right side (X in Figure 2) yields  $K\lambda/L$  as the slope and  $16e^2$  as the intercept of a linear relation from which L and e can be calculated.

## RESULTS AND DISCUSSION

The magnetic extract from the soil consisted of almost pure greigite with traces of pyrite (Figure 1). The sedimentary greigite contained traces of smyhtite and an additional, unidentified phase. The d-values of both soil and sedimentary greigites are significantly smaller

than those reported by Skinner *et al.* (1964) (Table 1), resulting in smaller cell edge lengths a of 9.8639(3) Å and 9.8737(4) Å compared with 9.876 Å (Skinner *et al.*, 1964), 9.859 Å (Giovanolli, 1979), and 9.88 Å (Vandenbergh *et al.*, 1991). The relative peak intensities of both greigites are identical within experimental errors and agree with the intensities given by Skinner *et al.* (1964), with the exception that 440 rather than 311 is the strongest reflection (Table 1). Because of low intensities, 331, 531, and 551 were not detected in the soil greigite.

The mean coherence lengths (MCL) and strain were calculated from the corrected integral widths of the X-ray peaks on the basis of Eq. (1). Using all peaks, the soil greigite had an MCL of  $23 \pm 2$  nm, whereas the sedimentary greigite had larger particles  $60 \pm 5$  nm in size. The regressions, however, are strongly influenced by the first peak (111), which a plot of Y vs. X shows to be far removed from all other peaks. Therefore, alternative calculations were carried out using series of peaks. For the hhh series, the MCLs are identical with the aforementioned values (Table 2). The series 220 + 440 and 400 + 800 gave lower coherence lengths, although the appropriate Scherrer constants should have compensated for different orientations of the diffracting planes relative to the (assumed) octahedral morphology of the crystals. The decrease of  $MCL_{hhh} > MCL_{hh0} > MCL_{h00}$  indicates for both greigites that the single crystallites are elongated along 111. This is supported by TEM observations, which show strong elongations for this soil greigite (Stanjek *et al.*, 1994). In all cases strain is negligibly small.

Table 1. d values and relative X-ray diffraction peak intensities of soil and sedimentary greigite.

hkl	Soil greigite			Sediment greigite		JCPDS 16-713	
	$d_{meas}$	$d_{calc}$	Intensity	$d_{meas}$	Intensity	$d_{meas}$	Intensity
111	5.693	5.695	5	5.703	5	5.72	8
220	3.483	3.487	18	3.489	21	3.50	30
311	2.9733	2.8741	75	2.9766	69	2.980	100
222	2.8448	2.8475	4	2.8490	6	2.855	4
400	2.4674	2.4660	66	2.4686	56	2.470	55
331	—	—	—	2.2662	<1	2.260	2
422	2.0124	2.0135	10	2.0153	8	2.017	10
333	1.8984	1.8983	21	1.9002	31	1.901	30
440	1.7430	1.7437	100	1.7454	100	1.746	75
531	—	—	—	—	—	1.671	<1
620	1.5626	—	4	1.5611	2	1.563	4
533	1.50431	1.50423	13	1.50540	11	1.506	10
622	1.48543	—	4	1.48808	3	1.488	2
444	1.42393	1.42373	12	1.42564	16	1.425	8
551	—	—	—	1.38206	3	1.383	<1
642	1.31804	1.31812	9	1.31929	6	1.320	4
731	1.28415	1.28417	12	1.28557	8	1.286	12
800	1.23303	1.23299	9	1.23411	6	1.235	10
Cell edge length a [Å]		9.8639 $\pm 0.0003$		9.8737 $\pm 0.0004$		9.876	

Data from Skinner *et al.* (1964) are included for comparison.

Table 2. Mean coherence lengths (MCL) of soil and sedimentary greigite.

Peaks	Soil		Sediment	
	MCL [nm]	Strain	MCL [nm]	Strain
All	23 ± 2	0.0012 ±0.0002	60 ± 5	0.0004 ±0.00006
111, 222, 333, 444	23 ± 1	0.0008 ±0.0002	59 ± 1	0.0003 ±0.00004
220, 440	20	0.0009	47	0.0003
400, 800	16	0.0014	38	0.0

The room-temperature Mössbauer spectra of both greigites (Figure 2) consist of two sextets with similar magnetic hyperfine fields (Table 3). The first sextet with similar hyperfine fields of 31.1 and 31.3 T and isomer shifts of 0.33 mm/s can be assigned to tetrahedral sites, whereas the second sextet with 30.7 T and 0.57 (0.60) mm/s isomer shift results from iron in the octahedral sites. In spite of structural equivalence to magnetite, the hyperfine fields of greigite are much lower, probably due to strong covalency effects. In contrast to the sedimentary sample, the spectrum of the soil greigite also shows a doublet with a high line width of 0.43 mm/s, which probably results from a superparamagnetic (SP) component. The sedimentary sample shows two additional weak sextets (Table 3) with magnetic fields of 24.7 and 24.4 T, which can be assigned to smythite (Hoffmann *et al.*, 1993). The two stronger sextets of smythite are obscured by the greigite sextets because of almost identical hyperfine fields and isomer shifts.

The observation of similar hyperfine fields for iron in both tetrahedral and octahedral sites is due to a pronounced temperature dependence of the hyperfine fields in greigite (Vandenberghe *et al.*, 1991). Although octahedrally coordinated iron in greigite has a higher saturation field than in tetrahedral coordination, the former decreases more rapidly as temperature is increased, and both hyperfine fields are equal at about 290 K. It is, however, probable that small particle size (as measured by X-ray diffraction) will also have an influence on the magnitude of the hyperfine fields. The lowest fields were observed for the soil greigite, intermediate fields for our sedimentary greigite, and the

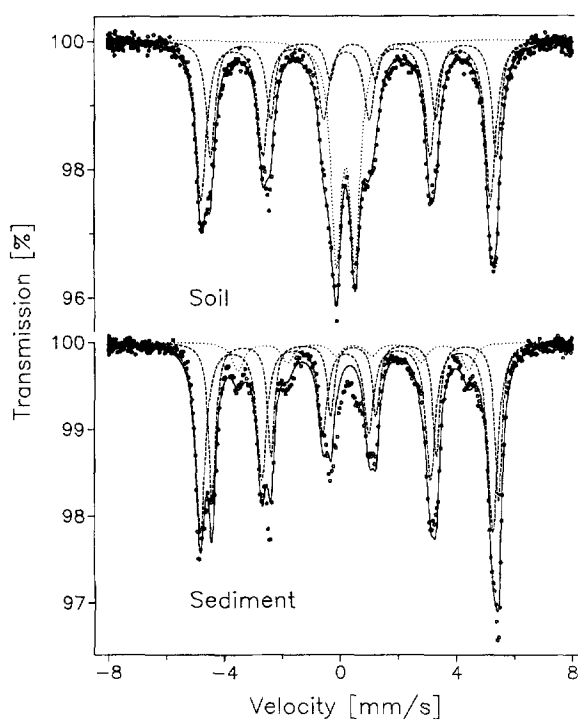


Figure 2. Room-temperature Mössbauer spectra of soil and sedimentary greigite. In both spectra dashed lines indicate sextets. The dotted line in the soil spectrum indicates the doublet, in the sediment spectrum the additional sextet (See Table 3).

highest fields for the sample described by Vandenberghe *et al.* (1991), which was reported to show relatively narrow X-ray diffraction lines.

The most interesting feature, however, is the fact that the soil and sedimentary greigite show magnetic order at room temperature, although their particle sizes lie within the region that is characteristic for SP behavior (Figure 3; Ricci and Kirschvink, 1992). This discrepancy has also been described for the macroscopic single-domain behavior (Stanjek *et al.*, 1994). It has been explained by the dense aggregation of greigite particles, which have different crystallographic orientation towards each other—hence giving small crystalline sizes in X-ray diffraction—but common magnetic orientations. If the relaxation time is changed from 100

Table 3. Room-temperature Mössbauer data.

Sample	Greigite: tetrahedral sites				Greigite: octahedral sites			
	$B_{\text{hf}}$ [T]	$\delta/\text{Fe}$ [mm/s]	$2\epsilon$ [mm/s]	$W$ [mm/s]	$B_{\text{hf}}$ [T]	$\delta/\text{Fe}$ [mm/s]	$2\epsilon$ [mm/s]	$W$ [mm/s]
Soil	31.1	0.33	-0.01	0.44	30.7	0.57	0.02	0.37
Sediment	31.3	0.33	0.02	0.39	30.7	0.60	0.08	0.29
Sediment <sup>1</sup>	31.3	0.28	0.0	—	31.3	0.53	-0.08	—

<sup>1</sup> Data (300 K) from Vandenberghe *et al.* (1991) for sedimentary greigite from the Sokolov Basin, Czechian Republik.

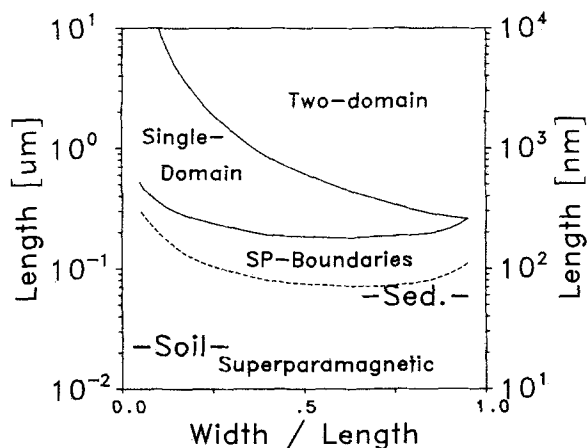


Figure 3. Single-domain stability diagram for different shapes of prolate spheroid grains of greigite (redrawn from Figure 1 of Ricci and Kirschvink, 1992). Boundaries between the superparamagnetic and the single-domain region are indicated for relaxation times of 100 s (upper curve) and of  $10^{-8}$  s (broken line). The approximate ratio of width/length has been inferred from the saturation magnetization values, which are given in Figure 1 of Ricci and Kirschvink, 1992.

s for macroscopic measurements to  $10^{-8}$  s for Mössbauer spectroscopy (dashed curve in Figure 3), both greigites still lie within the SP region. This behavior is similar to that of a ferrihydrite–organic matter association, in which Schwertmann and Murad (1988) observed an enhancement of magnetic coupling across the ferrihydrite crystallites after removal of the organic matter.

### CONCLUSIONS

From all measured parameters, crystallite size is the only parameter in which our soil greigite differs substantially from the sedimentary greigite. All other parameters—cell edge length, magnetic hyperfine field, quadrupole splitting, and isomer shift—show a decrease towards the soil greigite, but further measurements on more samples are necessary in order to elucidate the natural variance of both soil and sedimentary greigites.

### ACKNOWLEDGMENTS

We are indebted to M. Krs for providing the sedimentary greigite and to R. E. Vandenberghe (Gent) for helpful comments. This study has been supported by the Deutsche Forschungsgemeinschaft.

### REFERENCES

Auerswald, K., Stanjek, H., and Becher, H. H. (1992) Böden in Landschaftsausschnitten Bayerns IV. Bodenabfolge in

- Dogger—Lias—Sedimenten am Hesselberg: *Landwirtschaftliches Jahrbuch* **69**, 73–87.
- Berner, R. A. (1969) Migration of iron and sulfur within anaerobic sediments during early diagenesis: *Amer. J. Sci.* **267**, 19–42.
- De Wolf, P. M. and Visser, J. W. (1988) Absolute intensities—Outline of a recommended practice: *Powder Diff.* **3**, 202–204.
- Dell, C. I. (1972) An occurrence of greigite in Lake Superior sediments: *Amer. Mineral.* **57**, 1303–1304.
- Giovanoli, F. (1979) Die remanente Magnetisierung von Seesedimenten: Ph.D. thesis, FB Geowissenschaften, Eidgenössische Technische Hochschule, Zürich, 198 pp.
- Hoffmann, V. (1992) Greigite ( $\text{Fe}_3\text{S}_4$ ): Magnetic properties and first domain observations: *Phys. Earth Planet. Int.* **70**, 288–301.
- Hoffmann, V., Stanjek, H., and Murad, E. (1993) Mineralogical, magnetic and Mössbauer data of smyhtite ( $\text{Fe}_3\text{S}_{11}$ ): *Studia Geophys. Geodaet.* **37**, 366–381.
- Janik, L. M. and Raupach, M. (1977) An iterative, least-squares program to separate infrared absorption spectra into their component bands: *CSIRO Div. Soils Techn. Paper* **35**, 1–37.
- Jedwab, J. (1967) Minéralisation en greigite de débris végétaux d'une vase récente (Grote Geul): *Bull. Soc. Belge Geol. Paléont. Hydrol.* **76**, 27–38.
- Langford, J. I. and Wilson, A. J. C. (1978) Scherrer after sixty years: A survey and some new results in the determination of crystallite size: *J. Appl. Crystall.* **11**, 102–113.
- Klug, H. P. and Alexander, L. E. (1974) *X-ray Diffraction Procedures for Polycrystalline and Amorphous Materials*: J. Wiley & Sons, New York, 966 pp.
- Krs, M., Krsova, M., Pruner, P., Zeman, A., Novak, F., and Jansa, J. (1990) A petromagnetic study of Miocene rocks bearing micro-organic material and the magnetic mineral greigite (Sokolov and Cheb basins, Czechoslovakia): *Phys. Earth Planet. Int.* **63**, 98–112.
- Mann, S., Sparks, N. H. C., Frankel, R. B., Bazylnski, D. A., and Jannasch, H. W. (1990) Biomineralization of ferri-magnetic greigite ( $\text{Fe}_3\text{S}_4$ ) and iron pyrite ( $\text{FeS}_2$ ) in a magnetotactic bacterium: *Nature* **343**, 258–261.
- Ricci, J. C., Diaz, and Kirschvink, J. L. (1992) Magnetic domain state and coercivity predictions for biogenic greigite ( $\text{Fe}_3\text{S}_4$ ): A comparison of theory with magnetosome observations: *J. Geophys. Res.* **97**, 17309–17315.
- Schwertmann, U. and Murad, E. (1988) The nature of an iron oxide–organic iron association in a peaty environment: *Clay Miner.* **23**, 291–299.
- Skinner, B. J., Erd, R. C., and Grimaldi, R. F. (1964) Greigite, the thiospinel of iron: A new mineral: *Amer. Mineral.* **49**, 543–555.
- Snowball, I. F. (1988) The occurrence of greigite in the sediments of Loch Lomond: *J. Quater. Sci.* **3**, 121–125.
- Stanjek, H. (1991) Aluminium- und Hydroxylsubstitution in synthetischen und natürlichen Hämatiten: Ph.D. thesis, TU-München, Marie L. Leidorf, Buch am Erlbach, 200 pp.
- Stanjek, H., Fassbinder, J. W. E., Vali, H., Wägele, H., and Graf, W. (1994) Evidence of biogenic greigite (ferri-magnetic  $\text{Fe}_3\text{S}_4$ ) in soil: *Eur. J. Soil Sci.* **45**, 97–103.
- Vandenberghe, R. E., De Grave, E., de Bakker, P. M. A., Krs, M., and Hus, J. J. (1991) Mössbauer study of natural greigite: *Hyperfine Inter.* **68**, 319–322.

(Received 29 September 1993; accepted 26 February 1994; Ms. 2425)